

Crystal structure solution from experimentally determined atomic pair distribution functions

P. JUHÁS,^{a*} L. GRANLUND,^b S. R. GUJARATHI,^b P. M. DUXBURY^b AND

S. J. L. BILLINGE^{a,c}

^a*Department of Applied Physics and Applied Mathematics, Columbia University, New York, New York, 10027, USA,* ^b*Department of Physics and Astronomy, Michigan State University, East Lansing, Michigan, 48824, USA,* and ^c*Condensed Matter Physics and Materials Science Department, Brookhaven National Laboratory, Upton, New York, 11973, USA. E-mail: pj2192@columbia.edu*

(Received 0 XXXXXXXX 0000; accepted 0 XXXXXXXX 0000)

Abstract

The paper describes an extension of the Liga algorithm for structure solution from atomic pair distribution function (PDF), to handle periodic crystal structures with multiple elements in the unit cell. The procedure is performed in 2 separate steps - at first the Liga algorithm is used to find unit cell sites consistent with pair distances extracted from the experimental PDF. In the second step the assignment of atom species over cell sites is solved by minimizing the overlap of their empirical atomic radii. The procedure has been demonstrated on synchrotron x-ray PDF data from 16 test samples. The structure solution was successful for 14 samples including cases with enlarged super cells. The algorithm success rate and the reasons for failed cases are discussed together with enhancements that should improve its convergence and usability.

1. Introduction

Crystallographic methods of structure solution are the gold-standard for determining atomic arrangements in crystals including, in the absence of single crystals, structure solution from powder diffraction data (Pecharsky & Zavalij, 2005; David *et al.*, 2002). Here we show that crystal structure solution is also possible from experimentally determined atomic pair distribution functions (PDF) using the Liga algorithm that was developed for nanostructure determination (Juhás *et al.*, 2006; Juhás *et al.*, 2008). The PDF is the Fourier transform of the properly normalized intensity data from an isotropically scattering sample such as a glass or a crystalline powder. It is increasingly used as a powerful way to study atomic structure in nanostructured materials (Billinge, 2008; Egami & Billinge, 2003). Such nanostructures do not scatter with well defined Bragg peaks and are not amenable to crystallographic analysis (Billinge & Levin, 2007), but refinements of models to PDF data yield quantitatively reliable structural information (Proffen & Billinge, 1999; Farrow *et al.*, 2007; Tucker *et al.*, 2007). Recently *ab initio* structure solution was demonstrated from PDF data of small elemental clusters (Juhás *et al.*, 2006). Here we show that these methods can be extended to solve the structure of a range of crystalline materials.

Whilst it is unlikely that this kind of structure solution will replace crystallographic methods for well ordered crystals, this work demonstrates both that structure solution from PDF data can be extended to compounds, and that robust structure solutions are possible from the experimentally determined PDFs of a wide range of materials. We also note that there may be an application for this approach when the space-group of the crystal is not known, as the Liga algorithm does not make use of such symmetry information. In fact, the space group can be determined afterwards analyzing the symmetry of the solved electron density map (Palatinus & van der Lee, 2008). However, this approach is promising for the case where the local structure deviates from the

average crystallographic structure, as has been observed in a number of complex crystals, for example the magnetoresistive $\text{La}_{1-x}\text{Ca}_x\text{MnO}_3$ system (Qiu *et al.*, 2005; Božin *et al.*, 2006) or ferroelectric lead-based perovskites (Dmowski *et al.*, 2000; Juhas *et al.*, 2004). The PDF contains this local information due to the inclusion of diffuse scattering intensities in the Fourier transform and it is possible to focus the modeling on a specific length-scale when searching for matching structure models, allowing in principle structure solutions of local, intermediate, and long-range order to be obtained separately.

The procedure assumes a periodic system with known lattice parameters and stoichiometry, otherwise there is no information on location or symmetry of the atom sites in the unit cell. To solve the unit cell structure the technique constructs a series of trial clusters using the PDF-extracted distances. The tested structures are created with a direct use of distance information in the experimental data giving it significantly better performance than procedures that search by random structure updates such as Monte Carlo based minimization schemes (Juhás *et al.*, 2006; Juhás *et al.*, 2008).

2. Experimental procedures

The extended Liga procedure has been tested with experimental x-ray PDFs collected from inorganic test materials. Powder samples of Ag, BaTiO_3 , C-graphite, CaTiO_3 , CdSe, CeO_2 , NaCl, Ni, PbS, PbTe, Si, SrTiO_3 , TiO_2 (rutile), Zn, ZnS (sphalerite) and ZnS (wurtzite) were obtained from commercial suppliers. Samples were ground in agate mortar to decrease their crystallite size and improve powder averaging. The experimental PDFs were measured using synchrotron x-ray diffraction at the 6ID-D beamline of the Advanced Photon Source, Argonne National Laboratory using the x-ray energies of 87 and 98 keV. The samples were mounted using a thin kapton tape in a circular, 10 mm hole of a 1 mm thick flat plate holder, which was positioned in trans-

mission geometry with respect to the beam. The x-ray data were measured using the “Rapid Acquisition” (RA-PDF) setup, where the diffracted intensities were scanned by a MAR345 image plate detector, placed about 20 cm behind the sample (Chupas *et al.*, 2003). All measurements were performed at room temperature. The raw detector images were integrated using the Fit2D program (Hammersley, 1998) to reduce them to a standard intensity vs. 2θ powder data. The integrated data were then converted by the PDFgetX2 program (Qiu *et al.*, 2004) to experimental PDFs. The conversion to PDF was conducted with corrections for Compton scattering, polarization and fluorescence effect, as available in the PDFgetX2 program. The maximum value of the scattering wavevector Q_{\max} ranged from 19 \AA^{-1} to 29 \AA^{-1} , based on a visual inspection of the noise in the $F(Q) = Q[S(Q) - 1]$ curves.

The PDF function $G(r)$ was obtained by a Fourier transformation of $F(Q)$,

$$G(r) = \frac{2}{\pi} \int_{Q_{\min}}^{Q_{\max}} F(Q) \sin Qr \, dQ, \quad (1)$$

and provided a scaled measure of finding a pair of atoms separated by distance r

$$G(r) = \frac{1}{Nr \langle f \rangle^2} \sum_{i \neq j} f_i f_j \delta(r - r_{ij}) - 4\pi\rho_0 r. \quad (2)$$

The $G(r)$ function has a convenient property that its peak amplitudes and standard deviations remain essentially constant with r and is thus suitable for curve fitting. A detailed discussions of the PDF theory, data acquisition and applications for structure analysis can be found in (Egami & Billinge, 2003; Farrow & Billinge, 2009).

3. Methods

The structure solution procedure was carried out in three separate steps, as described in the sections below. The first step consists of peak search and profile fitting in the experimental PDF to identify prominent inter-atomic distances up to a cutoff distance d_{cut} . We have developed an automated peak extraction method which eases this task.

In the second step these distances are used as inputs for the Liga algorithm, which searches for unit cell positions that give structure with the best match in pair lengths. If the sample has several chemical species, a final “coloring” step is necessary to assign proper atom species to the unit cell sites. This can be done by making use of PDF peak amplitude information. However, we have found that coloring can be also solved by optimizing the overlap of the empirical atom radii at the neighboring sites, which is simpler to implement and works with greater reliability.

To verify the quality and uniqueness of the structure, the Liga algorithm has been run for each sample multiple (at least 10) times with the same inputs, but different seeds of the random number generator. For most samples the resulting structures were all equivalent, but sometimes the program gave several geometries with similar agreement to the PDF-extracted pair distances. In all these cases the correct structure could be resolved in the coloring step, where it displayed significantly lower atom radii overlap and converged to known structure solution. A small number of structures would not solve by this process and the reasons for failure are discussed below.

3.1. Extraction of pair distances from the experimental PDF

In the PDF frequent pair distances generate sharp peaks in the measured $G(r)$ curve with amplitudes following Equation (2). The peaks are broadened to approximately Gaussian shape that reflects atom thermal vibrations and limited experimental resolution. Additional broadening and oscillations are introduced to the PDF due to the maximum wavevector Q_{\max} that can be achieved in the measurement. This cutoff in Q_{\max} in effect convolutes ideal peak profiles with a sinc function $\sin(Q_{\max}r)/r$ thus creating satellite termination ripples.

Recovering the underlying peaks from the PDF is not trivial. The experimental curve can have false peaks due to termination ripples. Nearby peaks can overlap and

produce complicated profiles that are difficult to decompose. To simplify the process of extracting inter-atomic distances we have developed an automated method for peak fitting that adds peak profiles to fit the data to some user-defined tolerance, while using as few peaks as possible to avoid over-fitting. This method grows peak-like clusters of data points while fitting one or more model peaks to each cluster. Adjacent clusters iteratively combine until there is a single cluster with a model that fits the entire data set. This allows a steady growth in model complexity by progressively refining earlier and less accurate models. Furthermore, most adjustable parameters can be estimated, in principle, from experimental knowns. A full description of the peak extraction method will be presented in a future paper.

The present work uses the simplest model for peaks, fitting the $G(r)$ data with Gaussian peaks over r and using an assumed value of ρ_0 . This model ignores the effect of termination ripples, but for our data the spurious peaks due to these ripples were usually identifiable by their small size. Furthermore, the Liga algorithm is not required to use every distance it is given, and should exhibit a limited tolerance of faulty distances. The peak fitting procedure returns positions, widths and integrated areas of the extracted peaks, of which only the peak positions were used for structure determination.

The peak extraction procedure was implemented in Mathematica 6 and tested on both the experimental and simulated data. A typical runtime was about 5 minutes. Since the structures are known we can compare the results of the peak extraction with the expected results. For both experimental and simulated PDFs of the tested structures these compared qualitatively well to the ideal distances up to $\sim 10\text{-}15$ Å, including accurate identification of some obscured peaks. Past that range the number of distinct, but very close, distances in the actual structure is so great that reliable peak extraction is much more difficult. For this reason we only performed peak extraction up

to 10 Å before running the trials described in Section 4. Apart from removing peaks below a noise threshold in order to filter termination ripples out, and one difficult peak in the graphite data, all distances used in the structure solution trials below come directly from the peak extraction method.

3.2. Unit cell reconstruction using the Liga algorithm

In the second step the Liga algorithm searches for the atom positions in the unit cell that make the best agreement to the extracted pair distances. The quality of distance match is expressed by cost C_d defined as a mean square difference between observed and modeled pair distances.

$$C_d = \frac{1}{P} \sum_{d_k < d_{cut}} (t_{k, near} - d_k)^2 \quad (3)$$

The index k goes over all pair distances d_k in the model that are shorter than the cutoff length d_{cut} and compares them with the nearest observed distance $t_{k, near}$, while P is the number of model distances. This cost definition considers only distance values as extracted from the PDF peak positions, and ignores their relative occurrences. For multi-component systems there is in fact no straightforward way of extracting distance multiplicities, because it is not known what atom pairs are present in each PDF peak. Nevertheless, the cost definition still imposes strict requirements on the model structure, as displayed in Fig. 1. A site in the unit cell must be at a good, matching distance not only from all other cell sites, but also from all of their translational images within the cutoff radius.

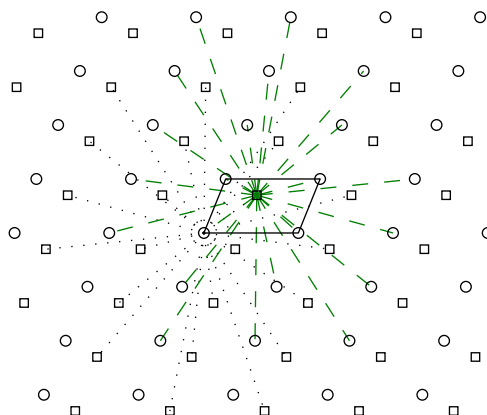


Fig. 1. Schematic calculation of the distance cost C_d . To achieve low C_d a unit cell site needs to be at a correct distance from other cell sites and from their translational images.

To find an optimum atom position in the unit cell structure the Liga algorithm uses input pair distances in an iterative build-up and disassembly of partial structures (Juhás *et al.*, 2006). The procedure maintains a pool of partial unit cell structures at each possible size from a single atom up to a complete unit cell. These “candidate clusters” are assigned to “divisions” according to the number of sites they contain, therefore there are as many divisions as is the number of atoms in a complete unit cell. The structures at each division compete against each other in a stochastic process, where the probability of winning equals the reciprocal distance cost C_d , and a win is thus more likely for low-cost structures. The winning cluster is selected for “promotion,” where it adds one or more atoms to the structure and thus advances to a higher division. At the new division a poorly performing high-cost candidate is “relegated” to the original division of the promoted structure, thus keeping the total number of structures at each division constant. The relegation is accomplished by removing cell sites that have the largest contributions to the total cost of the structure. Both promotion and relegation steps are followed by downhill relaxation of the worst site, i.e., the site with the largest share of the total cost C_d . The process of promotion and

relegation is performed at every division in a “season” of competitions. These seasons are repeated many times until a full sized structure attains sufficiently low cost or until a user-specified time limit. A complete description of the Liga algorithm details can be found in (Juhás *et al.*, 2008).

3.3. Atom assignment

The Liga algorithm used in the structure solution step has no notion of chemical species and therefore returns only coordinates of the atom sites in the unit cell. For a multi-component system an additional step, dubbed coloring, is necessary to assign chemical elements over known cell sites. To assess the quality of different assignments we have tested two definitions for a cost of a particular coloring. The first method uses a weighted residuum, R_w , from a least-squares PDF refinement to the input PDF data (Egami & Billinge, 2003). The PDF refinement was performed with a fully automated PDFfit2 script, where the atom positions were all fixed and only the atomic displacement factors, PDF scale factor and Q -resolution damping factor were allowed to vary. The second procedure defines coloring cost C_c as an average overlap of the empirical atomic radii, so that

$$C_c = \frac{1}{N} \sum_{d_k < r_{k,1} + r_{k,2}} (r_{k,1} + r_{k,2} - d_k)^2 \quad (4)$$

The index k runs over all atom pairs considering periodic boundary conditions, $r_{k,1}$ and $r_{k,2}$ are the empirical radii values of the first and second atom in the pair k , and N is the number of atoms in the unit cell.

Considering an N atom structure with s different atom species, the total number of possible assignments is given by the multinomial expression $N!/(n_1! n_2! \dots n_s!)$. For a 1:1 binary system the number of possible assignments tends to 2^N with increasing N . Such exponential growth in possible configurations makes it quickly impossible to compare them all in an exhaustive way. We have therefore employed a simple downhill

search, which starts with a random element assignment. The initial coloring cost C_c is calculated together with a cost change for every possible swap of two atoms between unit cell sites. The site flip that results in the largest decrease of the total coloring cost is accepted and all cost differences are evaluated again. The site swap is then repeated until a minimum configuration is achieved, where all site flips increase the coloring cost. The downhill procedure was verified by repeating it 5 times using different initial assignments. In nearly all cases these runs converged to the same atom configurations.

The downhill procedure was performed using both definitions of the coloring cost. For the coloring cost obtained by PDF fitting the procedure was an order of magnitude slower and less reliable, as the underlying PDF refinements could converge badly for poor atom assignments. The second method, which calculated cost from radii-overlap, was considerably faster and more robust. For all tested materials, the overlap-based coloring assigned all atoms correctly, when run on correct structure geometry. The overlap cost was evaluated using either the covalent radii by (Cordero *et al.*, 2008) or the ionic radii from (Shannon, 1976) for more ionic compounds. For some ions the Shannon table provides several radii values depending on their coordination number or spin state. Although these variants in ionic radii can vary by as much as about 30%, the choice of particular radius had no effect on the best assignment for all studied structures.

4. Results

The experimental x-ray PDFs were acquired from 16 test samples with well known crystal structures. To verify that the measured PDF data were consistent with established structure results structure refinements of the known structures were carried out using the PDFgui program (Farrow *et al.*, 2007). The PDF fits were done with structure data obtained from the Crystallography Open Database (COD) (Gražulis

et al., 2009). The structure parameters were all kept constant in the refinements, which modified only parameters related to the PDF extraction, such as PDF scale, Q resolution dampening envelope and a small rescaling of the lattice parameters. These refinements are summarized in Table 1, where low values of the fitting residual R_w confirm good agreement between experimental PDFs and expected structure results.

The PDF datasets were then subjected to the peak search, Liga structure solution and coloring procedures as described above. To check the stability of this method, several structures were solved using an enlarged periodicity of $1\times 1\times 2$, $1\times 2\times 2$ or $2\times 2\times 2$ super cells. The lattice parameters used in the Liga crystallography step were obtained from the positions of the nearest PDF peaks. In several cases, such as for BaTiO_3 where peak search could not resolve tetragonal splitting, the cell parameters were taken from the respective CIF reference, as listed in Table 1.

The structure solution was considered successful if the found structure displayed the same nearest neighbor coordination as its CIF reference and no site was offset by more than 0.3 \AA from its correct position. The solution accuracy was evaluated by finding the best overlay of the found structure to the reference CIF data. The optimum overlay was obtained by an exhaustive search over all symmetry operations defined in the CIF file and over all mappings of solved atom sites to all reference sites containing the same element. The overlaid structures were then compared for the differences in fractional coordinates and for the root mean square distortion s_r of the solved sites from their correct positions. Table 2 shows a summary of these results for all tested structures.

Table 1. *List of measured x-ray PDFs and their fitting residua R_w with respect to established structures from the literature.*

sample	R_w	CIF reference
Ag	0.095	(Wyckoff, 1963)
BaTiO ₃	0.123	(Megaw, 1962)
C (graphite)	0.248	(Wyckoff, 1963)
CaTiO ₃	0.083	(Sasaki <i>et al.</i> , 1987)
CdSe	0.149	(Wyckoff, 1963)
CeO ₂	0.098	(Wyckoff, 1963)
NaCl	0.161	(Jurgens <i>et al.</i> , 2000)
Ni	0.109	(Wyckoff, 1963)
PbS	0.085	(Ramsdell, 1925)
PbTe	0.070	(Wyckoff, 1963)
Si	0.085	(Wyckoff, 1963)
SrTiO ₃	0.143	(Mitchell <i>et al.</i> , 2002)
TiO ₂ (rutile)	0.146	(Meagher & Lager, 1979)
Zn	0.105	(Wyckoff, 1963)
ZnS (sphalerite)	0.102	(Skinner, 1961)
ZnS (wurtzite)	0.174 ¹	(Wyckoff, 1963)

¹ refined as mixture of wurtzite and sphalerite phases

The procedure converged to a correct structure for 14 out of 16 studied samples and failed to find the remaining 2. The convergence was more robust for high-symmetry structures, such as Ag (*f.c.c.*), NaCl or ZnS sphalerite, which could be reliably solved also in enlarged [222] supercells. For all successful runs the distance cost C_d of the Liga-solved structure was comparable to the one from the CIF reference and the atom overlap measure C_c was close to zero. ZnS sphalerite shows a notable difference between the C_d values of the solution and its CIF reference, however this was caused by using a PDF peak position as a cell parameter for the solved structure. Apparently the PDF peak extracted at $r \approx a$ was slightly offset with respect to other peaks, nevertheless the Liga algorithm still produced atom sites with correct fractional coordinates. The mean displacement s_r for ZnS is 0 Å, because solved structures and CIF references were compared using lattice parameters rescaled to their CIF values.

Table 2. Summary of tested structure solutions from x-ray PDF data

sample (supercell)	atoms	cost C_d (0.01 Å ²)		cost C_c (Å ²)		deviation of coordinates			s_r (Å)
		Liga	CIF	Liga	CIF	s_x	s_y	s_z	
successful solutions									
Ag [111]	4	0.0232	0.136	0	0.001	0	0	0	0
Ag [222]	32	0.0097	0.136	0	0.001	0.00025	0.00024	0.00003	0.0014
BaTiO ₃ [111]	5	0.370	0.394	0.040	0.042	0.0057	0.0066	0.014	0.064
BaTiO ₃ [112]	10	0.392	0.394	0.058	0.042	0.00023	0.039	0.018	0.16
C graphite [111]	4	0.396	0.574	0.010	0.016	0.0029	0.0029	0.036	0.14
C graphite [221]	16	0.420	0.574	0.010	0.016	0.0086	0.0065	0.036	0.15
CdSe [111]	4	0.107	0.138	0	0.001	0	0	0.0055	0.027
CdSe [221]	16	0.0856	0.138	0	0.001	0.00010	0.00013	0.0057	0.028
CeO ₂ [111]	12	0.515	0.554	0	0	0	0	0	0
NaCl [111]	8	1.75	1.71	0	0	0	0	0	0
NaCl [222]	64	1.20	1.71	0	0	0.00031	0.00031	0.00035	0.0032
Ni [111]	4	0.0024	0.0024	0	0	0	0	0	0
Ni [222]	32	0.0025	0.0024	0	0	0.00015	0.00013	0.00013	0.0008
PbS [111]	8	0.0125	0.0104	0.010	0.011	0	0	0	0
PbS [222]	64	0.0140	0.0104	0.010	0.011	0.00005	0.00004	0.00005	0.0005
PbTe [111]	8	0.0024	0.0127	0.097	0.090	0	0	0	0
PbTe [222]	64	0.0022	0.0127	0.097	0.090	0.00011	0.00011	0.00008	0.0011
Si [111]	8	0.0045	0.0045	0	0	0	0	0	0
Si [222]	64	0.0048	0.0045	0	0	0.00010	0.00009	0.00008	0.0009
SrTiO ₃ [111]	5	0.437	0.437	0.002	0.002	0	0	0	0
Zn [111]	2	0.495	0.470	0	0	0	0	0.027	0.095
Zn [222]	16	0.564	0.470	0	0	0.00010	0.00006	0.020	0.080
ZnS sphalerite [111]	8	0.150	0.0647	0	0	0	0	0	0
ZnS sphalerite [222]	64	0.160	0.0647	0	0	0.00029	0.00033	0.00031	0.0028
ZnS wurtzite [111]	4	0.141	0.152	0	0	0	0	0.0038	0.017
ZnS wurtzite [221]	16	0.165	0.152	0	0	0.00003	0.00002	0.0039	0.017
failed solutions									
CaTiO ₃ [111]	20	0.4967	0.902	0.52	0.072	0.16	0.14	0.17	1.6
TiO ₂ rutile [111]	6	0.5358	0.758	0.40	0.009	0.081	0.24	0.00004	0.94

C_d, C_c – distance and atom overlap cost as defined in equations (3), (4)
 s_x, s_y, s_z – standard deviation in fractional coordinates normalized to a simple [111] cell
 s_r (Å) – root mean square displacement of the solved sites from the reference CIF positions

The structure determination did not work for 2 lower-symmetry samples of CaTiO₃ and TiO₂ rutile. In both of these cases, the simulated structure showed significantly lower distance cost C_d while its atom overlap C_c was an order of magnitude higher than for the correct structure and clearly indicated an unphysical result. Such results were caused by a poor quality of the extracted distances, which contained significant

errors and omissions with respect to an ideal distance list. The peak search and distance extraction is more difficult for lower symmetry structures, because their pair distances are more spread and produce small features that can be below the technique resolution. Because of poor distance data, the Liga algorithm converged to incorrect geometries that actually displayed a better match with the input distances. Both CaTiO_3 and TiO_2 were easily solved when run with ideal distances calculated from the CIF structure.

The results in Table 2 suggest several ways to extend the method and improve its success rate. First, the Liga geometry solution and coloring steps can be performed together, in other words the structure coloring step needs to be merged to a chemistry aware Liga procedure. Since atom overlap cost C_c is meaningful and can be easily evaluated for partial structures, the total cost minimized by the Liga algorithm should equal a weighted sum of C_c and distance cost C_d . Such a cost definition would steer the Liga algorithm away from faulty structures found for CaTiO_3 and TiO_2 rutile, because both of them had huge atom overlaps C_c . Another improvement is to perform PDF refinement for a full sized structure and update its cost formula so that the PDF fit residuum R_w is used instead of distance cost C_d . Such modification would prevent the cost advantage for wrong structures due to errors and omissions in the extracted distances. The assumption is that the distance data are still good enough to let the Liga algorithm construct the correct structure in one of its many trials. Finally, the cost definition for partial structures can be enhanced with other structural criteria such as bond valence sums (BVS) agreement (Brese & Okeeffe, 1991; Norberg *et al.*, 2009). Bond valence sums are not well determined for incomplete intermediate structures and thus cannot fully match their expected values. However, BVS are always increasing, therefore a BVS of some ion that is significantly larger than its expected value is a clear sign of such a partial structure's poor quality.

5. Conclusions

We have demonstrated the Liga algorithm for structure determination from PDF can be extended from its original scope of single-element non-periodic molecules (Juhás *et al.*, 2006; Juhás *et al.*, 2008) to multi-component crystalline systems. The procedure assumes known lattice parameters and it solves structure geometry by optimizing pair distances to match the PDF extracted values, while the chemical assignment is obtained from minimization of the atomic radii overlap. The procedure was tested on x-ray PDF data from 16 test samples, of which in 14 cases it gave the correct structure solution. These are promising results, considering the technique is at a prototype stage and will be further developed to improve its ease of use and rate of convergence. The procedure can be easily amended by a final PDF refinement step. Such an implementation could significantly reduce the overhead in PDF analysis of crystalline materials, because its most difficult step, a design of suitable structure model, would become fully automated.

Acknowledgements

We gratefully acknowledge Dr. Emil Božin, Dr. Ahmad Masadeh and Dr. Douglas Robinson for help with x-ray measurements at the Advanced Photon Source at the Argonne National Laboratory (APS, ANL). We thank Dr. Christopher Farrow for helpful suggestions and consultations and Dr. Christos Malliakas for providing NaCl and ZnS wurtzite samples. We appreciate the computing time and support at the High Performance Computing Center of the Michigan State University, where we performed all calculations. This work has been supported by the National Science Foundation (NSF) Division of Materials Research through grant DMR-0520547. Use of the APS is supported by the U.S. DOE, Office of Science, Office of Basic Energy Sciences, under Contract No. W-31-109-Eng-38. The 6ID-D beamline in the MUCAT sector at the APS is supported by the U.S. DOE, Office of Science, Office of Basic Energy Sciences,

through the Ames Laboratory under Contract No. W-7405-Eng-82.

References

- Billinge, S. J. L. (2008). *J. Solid State Chem.* **181**, 1698–1703.
- Billinge, S. J. L. & Levin, I. (2007). *Science*, **316**, 561–565.
- Božin, E. S., Qiu, X., Schmidt, M., Paglia, G., Mitchell, J. F., Radaelli, P. G., Proffen, T. & Billinge, S. J. L. (2006). *Physica B*, **385-386**, 110–112.
- Brese, N. E. & Okeeffe, M. (1991). *Acta Crystallogr. B*, **47**(2), 192–197.
- Chupas, P. J., Qiu, X., Hanson, J. C., Lee, P. L., Grey, C. P. & Billinge, S. J. L. (2003). *J. Appl. Crystallogr.* **36**, 1342–1347.
- Cordero, B., Gomez, V., Platero-Prats, A. E., Reyes, M., Echeverria, J., Cremades, E., Barragan, F. & Alvarez, S. (2008). *Dalton T.* (21), 2832–2838.
- David, W. I. F., Shankland, K., McCusker, L. B. & Baerlocher, C. (eds.) (2002). *Structure Determination from Powder Diffraction Data*. Oxford: Oxford University Press.
- Dmowski, W., Akbas, M. A., Davies, P. K. & Egami, T. (2000). *J. Phys. Chem. Solids*, **61**(2), 229–237.
- Egami, T. & Billinge, S. J. L. (2003). *Underneath the Bragg peaks: structural analysis of complex materials*. Oxford, England: Pergamon Press, Elsevier.
- Farrow, C. L. & Billinge, S. J. L. (2009). *Acta Crystallogr. A*, **65**(3), 232–239.
- Farrow, C. L., Juhás, P., Liu, J. W., Bryndin, D., Božin, E. S., Bloch, J., Proffen, T. & Billinge, S. J. L. (2007). *J. Phys.: Condens. Mat.* **19**, 335219.
- Gražulis, S., Chateigner, D., Downs, R. T., Yokochi, A. F. T., Quirós, M., Lutterotti, L., Manakova, E., Butkus, J., Moeck, P. & Le Bail, A. (2009). *J. Appl. Crystallogr.* **42**(4).
- Hammersley, A. P. (1998). Fit2d v9.129 reference manual v3.1. ESRF Internal Report ESRF98HA01T.
- Juhás, P., Cherba, D. M., Duxbury, P. M., Punch, W. F. & Billinge, S. J. L. (2006). *Nature*, **440**(7084), 655–658.
- Juhás, P., Granlund, L., Duxbury, P. M., Punch, W. F. & Billinge, S. J. L. (2008). *Acta Crystallogr. A*, **64**(6), 631–640.
- Juhas, P., Grinberg, I., Rappe, A., Dmowski, W., Egami, T. & Davies, P. (2004). *Phys. Rev. B*, **69**(21), 214101.
- Jurgens, B., Irran, E., Schneider, J. & Schnick, W. (2000). *Inorg. Chem.* **39**(4), 665–670.
- Meagher, E. P. & Lager, G. A. (1979). *Can. Mineral.* **17**(1), 77–85.
- Megaw, H. D. (1962). *Acta Crystallogr.* **15**, 972–973.
- Mitchell, J., Ling, C., Millburn, J., Argyriou, D., Berger, A., Medarde, M., Miller, D. & Luo, Z. (2002). *Appl. Phys. A - Mater.* **74**, S1776–S1778.
- Norberg, S. T., Tucker, M. G. & Hull, S. (2009). *J. Appl. Crystallogr.* **42**(2), 179–184.
- Palatinus, L. & van der Lee, A. (2008). *J. Appl. Crystallogr.* **41**, 975–984.
- Pecharsky, V. K. & Zavalij, P. Y. (2005). *Fundamentals of Powder Diffraction and Structural Characterization of Materials*. New York, USA: Springer.
- Proffen, T. & Billinge, S. J. L. (1999). *J. Appl. Crystallogr.* **32**, 572–575.
- Qiu, X., Th. Proffen, Mitchell, J. F. & Billinge, S. J. L. (2005). *Phys. Rev. Lett.* **94**, 177203.
- Qiu, X., Thompson, J. W. & Billinge, S. J. L. (2004). *J. Appl. Crystallogr.* **37**, 678.
- Ramsdell, L. S. (1925). *American Mineralogist*, **10**(9), 281–304.
- Sasaki, S., Prewitt, C. T., Bass, J. D. & Schulze, W. A. (1987). *Acta Crystallogr. C*, **43**, 1668–1674.
- Shannon, R. D. (1976). *Acta Crystallogr. A*, **32**, 751,767.
- Skinner, B. J. (1961). *American Mineralogist*, **46**(11-2), 1399–1411.
- Tucker, M. G., Keen, D. A., Dove, M. T., Goodwin, A. L. & Hui, Q. (2007). *J. Phys.: Condens. Mat.* **19**, 335218.
- Wyckoff, R. W. G. (1963). *Crystal Structures*, vol. 1. New York: Wiley, 2nd ed.